Tetrahedron Vol. 43, No. 7, pp. 1253 to 1272, 1987
Printed in Great Britain.

0040-4020/87 $3.00+.00
Pergamon Journals Ltd.

REACTION SELECTIVITY IN SOLID STATE PHOTOCHEMISTRY

SARA ARIEL, SYED ASKARI, STEPHEN V. EVANS, CHRISTINE HWANG, JACK JAY, JOHN R. SCHEFFER*, JAMES TROTTER*, LEUEEN WALSH, and YIU-FAI WONG

The University of British Columbia, Department of Chemistry, 2036 Main Mall, Vancouver, B.C. Canada V6T 1Y6

(*Received in UK* 16 *February* 1987)

Steric compression, arising from intermolecular or intramolecular H...H non-bonded repulsive interactions generated along the reaction pathway, is used to explain abnormal solid state photoreactivity. Computer simulations of the motions involved in each case, with calculations of the resulting non-bonded steric compression energies were performed. Three systems were studied: (A) Enone photorearrangements, where the observed changes in the solid state photoreactivity of eight closely related a,β-unsaturated cyclohexenones are correlated with their crystal and molecular structures as determined by X-ray diffraction methods. (B) Failure of [2+2] photocycloaddition of an α,β-unsaturated ketone when irradiated in the solid state despite an almost perfect crystal lattice alignment of the potentially reactive double bonds. (C) An unsymmetrically substituted ene-dione for which solution photoreaction results in four products and solid state photoreaction yields only one.

Solid state photodimerization of cinnamic acid and its derivatives, studied in 1964 by Cohen and Schmidt[1], led to the formulation of the topochemical principle, which states that reactions in crystals tend to be least motion in character. In 1975 Cohen defined the "reaction cavity" as the space occupied by the reacting species and bounded by the surrounding stationary molecules[2]. It is well established that there is a preference for chemical processes to occur with minimal distortion of the "reaction cavity" (Figure 1).

This qualitative concept was tested quantitatively by McBride[3] and Gavezzoti[4]. McBride explained the details of the decomposition of diacyl peroxides in the solid state. Gavezzoti applied theoretical analysis to certain solid state processes in terms of the empty and filled volume spaces in the crystal lattice, concluding that "a prerequisite for crystal reactivity is the availability of free space around the reaction site."

Our aim was to identify specific steric interactions which alter reactivity in the solid state and to estimate their magnitude. For this reason we gathered information on three systems: (A) α,β-unsaturated ketones of general structure 1 (next page). In this series, we recently observed a photorearrangement which did not conform to the normal reactivity observed for these systems in the solid state and which could not be accounted for using traditional stereoelectronic arguments. This change in reactivity is explained here by specific crystal packing effects near the reaction site which are unique to the compound which behaves abnormally. (B) α,β-unsaturated ketone 2. This compound fails

to undergo [2+2] photocycloaddition when irradiated in the solid state despite an almost perfect crystal lattice alignment of the potentially reactive double bonds.
(C) unsymmetrically substituted ene-dione 3. Solid state photochemistry of this compound was expected to yield two photoproducts, based on the behaviour of similar homologues. However, irradiation of a crystalline sample of 3 results in only one product.

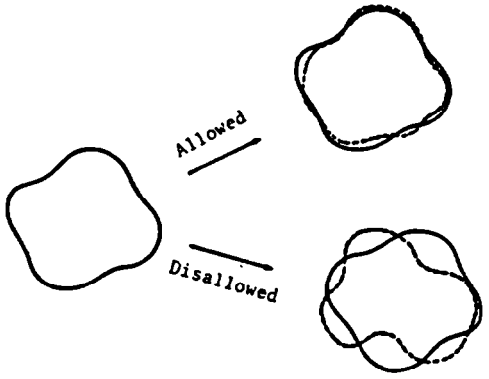

Figure 1. The reaction cavity concept in solid state chemistry (Cohen, 1975).
Full line - reaction cavity before reaction.
Broken line - transition state requirements for reaction.

All the structure-reactivity information gathered in this paper is based on photochemical and crystallographic studies performed in our laboratory over the last few years. The term "steric compression control" was suggested to explain the irregular solid state photochemical behavior[5]. Intermolecular steric hindrance was found to change reactivity for a unimolecular photorearrangement (example A) and for a bimolecular reaction (example B). Intramolecular steric compression was found to explain the solid state photochemical regioselectivity for example C (unimolecular). In each case the particular interactions affecting the reactivity were isolated and their magnitudes were estimated with use of non-bonded repulsive energy calculations.

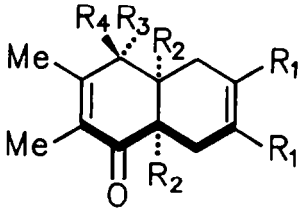

1

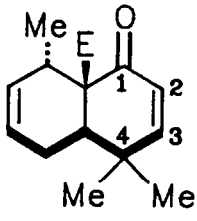

(E = $COOCH_3$)

2

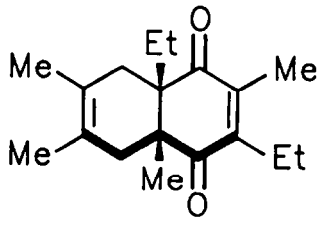

3

Intermolecular Steric Compression

(A) UNIMOLECULAR REACTION

Enone Photorearrangements

Enones of general structure 1, when irradiated in the crystalline phase, undergo one of two possible photorearrangements (path A or path B, Figure 2), both of which are initiated by intramolecular allylic hydrogen atom transfer to the β-carbon atom of the enone moiety, followed by closure of the resulting biradical species 4 or 5. Whether path A, leading to 4, or path B, leading to 5, is followed, depends upon the enone conformation adopted in the solid state[6]. Table I outlines the eight compounds, 1a-1h, studied; each has had its molecular and crystal structure determined by X-ray diffraction methods[7-12]. However, crystals of enone 1b are photochemically inert, and, most remarkably, irradiation of enone 1g in the solid state leads, via allylic hydrogen transfer to the enone α-carbon atom, to biradical 6g (path C). The photochemical reactions of enones 1a-1h are true solid state processes and not the result of photochemistry occurring in liquid regions of the crystal, as their irradiation in solution affords exclusively intramolecular [2+2] photocycloaddition[6].

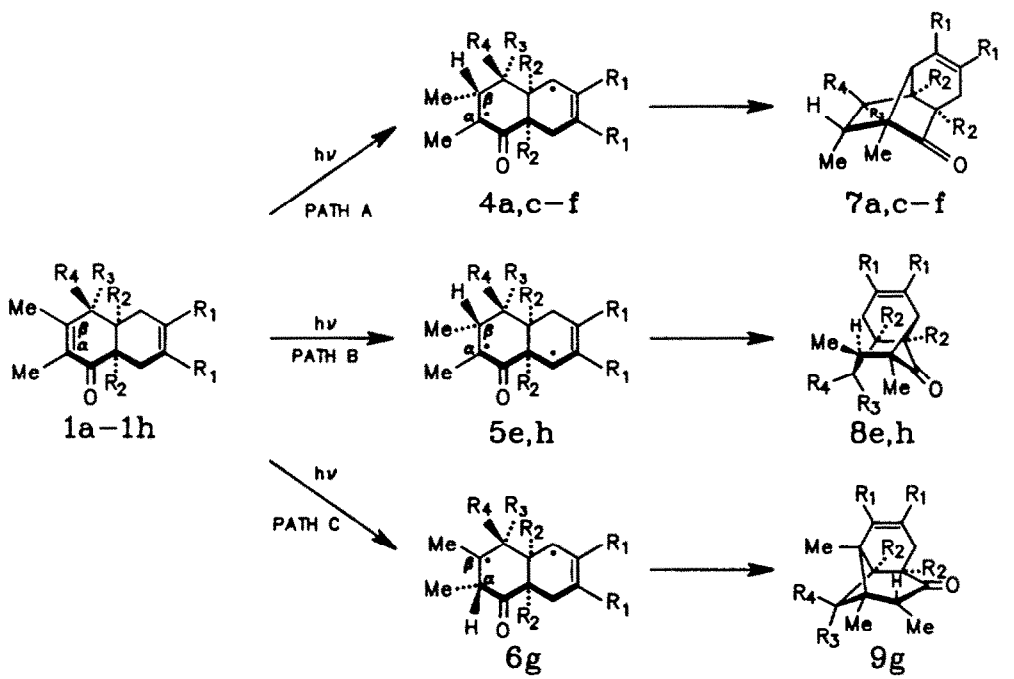

Figure 2. Possible reaction pathways for irradiation of compound 1 in the solid state.

Abstraction by the β-carbon of enones is normally preferred in solution photochemistry, and this is the regioselectivity followed in six of the eight compounds studied in this work. This can be attributed to the preference for forming a resonance-stabilized radical center next to the carbonyl group (4 and 5) rather than a radical which is not conjugated with the carbonyl group (6). The C...H distances summarized in Table I show no trend between ground state abstraction distance and preferred reactivity.

Inspection of the crystal packing for enones 1a-1h revealed that the change in hybridization of Cα or Cβ from sp^2 to sp^3, which necessarily accompanies hydrogen transfer to

Table I. Reactants, Hydrogen Abstraction Distances and Steric Compression in Solid State Photorearrangements.

Enone	R_1	R_2	R_3	R_4	H...Cα (Å)	H...Cβ (Å)	Steric Compression Accompanying Pyramidalization[1] Cα	Cβ	Intermolecular H...H Contacts (Å) Accompanying Pyramidalization[3] Cα	Cβ	and Methyl Rotations[4] Cα	Cβ
1a	CH_3	CH_3	H	OH	2.78	2.75	yes	yes	1.49	1.29	worse	1.88(42°S)
1b	CH_3	CH_3	OH	H	2.88[2]	2.92[2]	yes	yes	1.22	1.52	1.72(48°S)	worse
1c	CH_3	CH_3	OH	CH_3	2.86	2.81	yes	yes	1.55	1.28	1.96(50°P)	1.70(27°S)
1d	H	CH_3	H	OH	2.82	2.78	yes	no	1.24	>2.20	worse	not checked
1e	H	CH_3	OH	H	2.74	2.85	yes	yes	1.92**	1.59	worse	2.50(10°S)
1f	H	H	H	OH	2.92	2.84	yes	yes	1.82*	1.56	[5]	1.79(22°S)
1g	CH_3	CH_3	H	OAc	2.74	2.70	no	yes	>2.20	1.71	not checked	worse
1h	CH_3	CH_3	OAc	H	2.79	2.84	yes	yes	1.66	1.48	1.76(20°S)	1.79(53°S)

[1] Yes indicates a H...H contact upon pyramidalization of <1.9Å. In some cases more than one contact is developed. No indicates no contacts <2.2Å.

[2] Enone 1b does not react when photolyzed in the solid state.

[3] The intermolecular H...H contacts reported correspond to the shortest contact developed upon partial pyramidalization at 33° (marked with **), at 44° (marked with *); all others correspond to full pyramidalization at 55°.

[4] The intermolecular H...H distances reported here are of the best relieved contacts obtained by rotating either the stationary methyl groups (S) or the pyramidalized methyl groups (P). The angle of rotation, and the type of rotation (S or P) leading to the best relieved contact is reported in brackets.

[5] The 1.82Å contact is relieved by Me rotation after being first more sterically hindered. Since 1f reacts via β-abstraction, no details are given.

these atoms, would force the methyl groups at these centers into closer contacts with certain hydrogen atoms on neighboring molecules and thus sterically impede the reaction. Twisting about the carbon-carbon double bond, which is believed to accompany photoexcitation of α,β-unsaturated ketones in solution[13,14], does not seem to release this non-bonded strain. The steric hindrance to pyramidalization is represented schematically in Figure 3. The packing diagrams indicate that steric hindrance to pyramidalization (steric compression) is present in all eight compounds studied. For enones 1(a-c,e-f,h) steric compression occurs upon pyramidalization at both Cα and Cβ. The only exceptions to this trend were the Cα methyl group of compound 1g and the Cβ methyl group of enone 1d, for which pyramidalization appeared to be unimpeded. Therefore it appears that it is the void space surrounding the Cα methyl group of enone 1g which allows reaction and pyramidalization at this center in contrast to the steric compression which would attend reaction and pyramidalization at Cβ.

This hypothesis was tested by computer simulation along the pyramidalization pathway at either Cα or Cβ of a single molecule surrounded by its stationary lattice neighbors. With use of the X-ray crystal structure-derived coordinates of enones 1a-1h as a starting point, the methyl groups attached to Cα and Cβ were rotated out of the enone plane by intervals of 11°, 22°, 33°, 44° and 55° keeping all other molecular coordinates unchanged. Cα-CH_3 was rotated around an imaginary axis passing through Cα, perpendicular to the Cα-CH_3 bond and coplanar with the enone moiety.

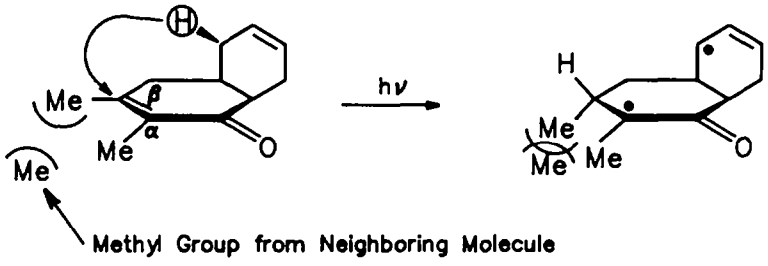

Figure 3. Steric compression accompanying pyramidalization at Cβ.

The same precedure was applied to the Cβ-CH_3. A rotation of 55° represents complete pyramidalization of the enone carbon atom. The direction of the rotation is away from the hydrogen being abstracted. The coordinates of the rotated methyl group were calculated by a local program. At each interval all contacts were calculated with the computer program INDIS3[15] which calculates inter- and intramolecular distances; any new H...H contacts of less than 2.2Å involving the computer-generated methyl groups were noted. The distance of 2.2Å was selected because this is the distance below which the nonbonded repulsion energy between hydrogen atoms becomes significant (vida infra).

The results confirmed that pyramidalization at Cα of enone 1g and Cβ of 1d led to no significant steric compression (contacts > 2.2Å), whereas pyramidalization in all other cases led to new intermolecular contacts averaging (at their minimum) 1.6 ± 0.3Å. These results are summarized in Table I. As an example, Figure 4 shows diagrams of enone 1g before and after pyramidalization at Cβ. The steric compression accompanying full 55° pyramidalization is indicated by the dotted lines and consists of H...H contacts of 1.71 and 1.87Å; pyramidalization of Cα is unimpeded.

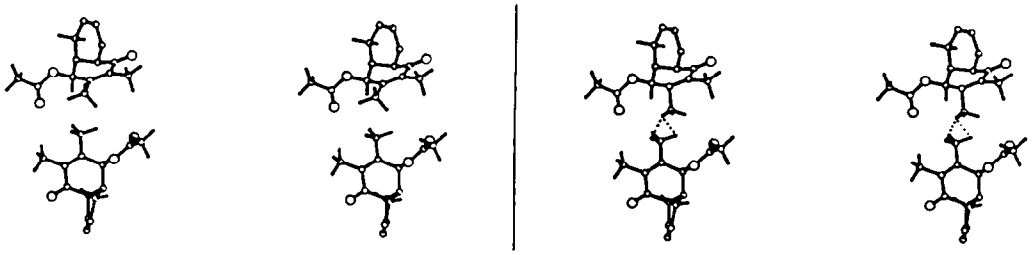

Figure 4. Computer simulation of pyramidalization at Cβ of enone 1g.
Left - before pyramidalization (no contacts < 2.2Å).
Right - after complete pyramidalization (dotted lines represent the new contacts at 1.71 and 1.87Å).

In order to estimate the steric compression energies accompanying pyramidalization, we used two of the better-known semi-empirical equations which relate interatomic distance and non-bonded repulsion energy. These are the Lennard-Jones 6-12 potential function as parameterized by Hagler and Sharon for their CMIN2 program[16]:

$$V_{6-12}(r)=0.038[2(2.75/r)^{12}-3(2.75/r)^{6}];$$

and the Buckingham potential as parameterized by Allinger for his MMP2 force field program[17],

$$V(r)=0.047[2.9\cdot10^{5}\cdot e^{-4.17r}-2.25(3/r)^{6}].$$

In both cases the parameters presented are for H...H interactions. These two functions are plotted graphically in Figure 5 for interactions involving hydrogen atoms. Using this plot we can estimate the steric compression energy for enone 1g fully pyramidalized at Cβ (contacts of 1.71 and 1.87Å). This amounts to 11.7 kcal/mole (MMP2) or 12.7 kcal/mole (CMIN2).

Methyl group rotation, which can be rapid in the solid state, can obviously alter the steric compression contacts. Initially, the computer simulation of pyramidalization was carried out keeping the methyl groups in their original ground state rotational orientations. Having determined the minimum intermolecular contacts attending pyramidalization, we then rotated the interacting methyl groups in both directions by 30° and determined the new intermolecular H...H contacts. The Cα methyl group was rotated around the pyramidalized $C\alpha-CH_3$ bond, clockwise and counterclockwise, in intervals of 10°; the Cβ methyl group was rotated around the pyramidalized $C\beta-CH_3$ bond. The rotation was carried out at the pyramidalized position corresponding to minimum intermolecular H...H contact for each case; i.e. at the most severe steric compression (thus not always at the geometry of complete pyramidalization). For each compound the methyl rotation calculation was carried out also for the stationary molecule which impeded the pyramidalization of the reacting molecule. The coordinates of the rotated methyl groups were calculated using the local program mentioned

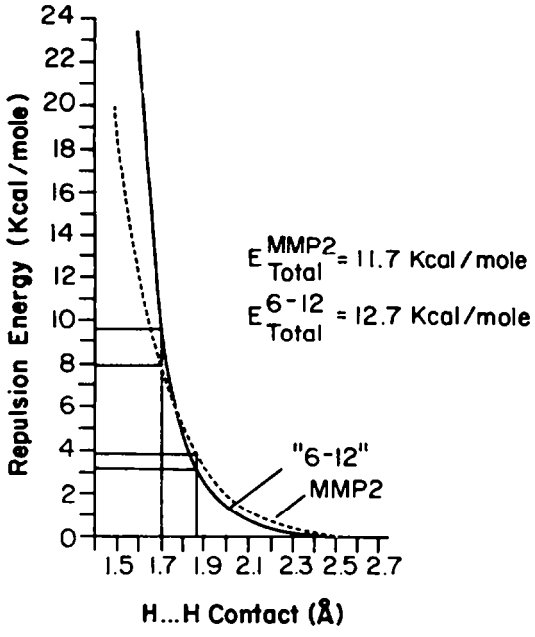

Figure 5. H...H non-bonded repulsion energy vs. distance. The details given are for steric compression energy arising after full pyramidalization at Cβ at enone 1g.

before. The new nonbonded H...H interactions arising from the methyl rotations were calculated for both independent and simultaneous rotations. The results of such a computer experiment for rotation are summarized in Table I. The detailed results of the rotation of the pyramidalized Cβ methyl group of enone 1g are given in Figure 6, which is a plot of intermolecular H...H contact versus angle of rotation. This shows that rotation of this methyl group in either direction does not relieve the steric compression caused by pyramidalization. For example, rotation in the positive direction, while slightly relieving the 1.71Å contact, strongly decreases the 1.87Å contact. Rotation in the opposite direction is no better; the 1.71Å contact is decreased slightly while the 1.87Å is relieved, but in addition, a third contact, 2.2Å, which is unimportant at 0°, becomes significant at approximately -20°. A similar rotation simulation was carried out for the stationary methyl group of the interacting pair in the case of enone 1g. Again, rotation was found to be ineffective in relieving the H...H steric compression contacts. Methyl rotation was tested for all eight enones studied. Although the H...H contacts varied with rotation (as above), in no case did rotation alter the conclusions reached on the basis of the 0° rotation contacts.

In Figure 7 we interpret the steric compression results kinetically in terms of the relative activation energies for hydrogen atom transfer. It is well established that hydrogen abstraction is the rate determining step in other hydrogen transfer-initiated photorearrangemnts such as the Norrish type II reaction[18-22]. In the absence of any steric compression, hydrogen abstraction by the β-carbon has a lower activation energy than hydrogen transfer to the α-carbon atom for reasons already discussed. Steric compression accompanying hydrogen transfer to both Cα and Cβ raises both activation energies, but maintains the ordering of Cβ below Cα [enones 1(a-c,e-f,h)]. Steric compression at Cα but not Cβ (enone 1d)

increases the normal activation energy difference resulting in abstraction by Cβ being even more favored than before. In the anomalous case of enone 1g, however, steric compression occurs only at Cβ with the result that abstraction by Cβ has a higher activation energy than abstraction by Cα, thus accounting for the observed change in regioselectivity. The photochemical inertness of enone 1b, which was originally ascribed solely to the long hydrogen abstraction distances involved[6] (2.88Å to Cα, and 2.92Å to Cβ, Table I), is due in addition to the severe steric compression which would accompany abstraction at either carbon, as the shortest intermolecular H...H contact resulting from pyramidalization was found for pyramidalized Cα of enone 1b (Table I).

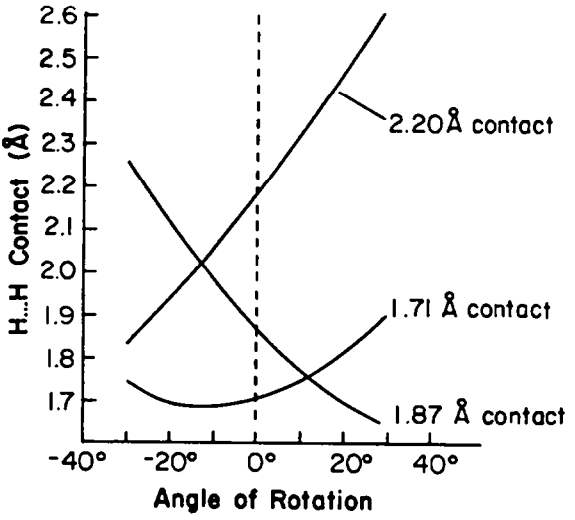

Figure 6. H...H contact vs. angle of rotation for the methyl group attached to the pyramidalyzed β-carbon atom of enone 1g.

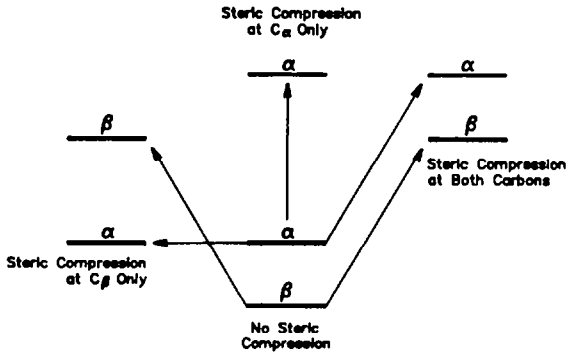

Figure 7. Relative activation energies for H-transfer to Cα and Cβ.

Calculation of the actual activation energy differences for each enone based on the H...H contacts developed during pyramidalization is not useful because of the relatively large (but normal) experimental errors in determining the hydrogen atom coordinates from the room temperature crystallographic data. As is apparent from Figure 5, compression energy is a very sensitive function of distance below 2Å.

(B) BIMOLECULAR REACTION

Inhibition of [2+2] Photocycloaddition

Following the pioneering work of Schmidt and co-workers on the solid state photodimerization reactions of the cinnamic acids[23], a very large amount of experimental evidence has accumulated which demonstrates that intermolecular [2+2] photocycloaddition is the virtually inevitable result of a crystal packing arrangement which orients lattice neighbors so that the potentially reactive double bonds are parallel at center-to-center distances of 4.1Å or less[24-31]. We were thus very surprised to observe the complete lack of photochemical reactivity of enone 2 when irradiated in the solid state. Compound 2 crystallizes in a lattice arrangement which is ideal for intermolecular [2+2] photocycloaddition[32] (Figure 8). The potentially reactive double bonds are oriented in a

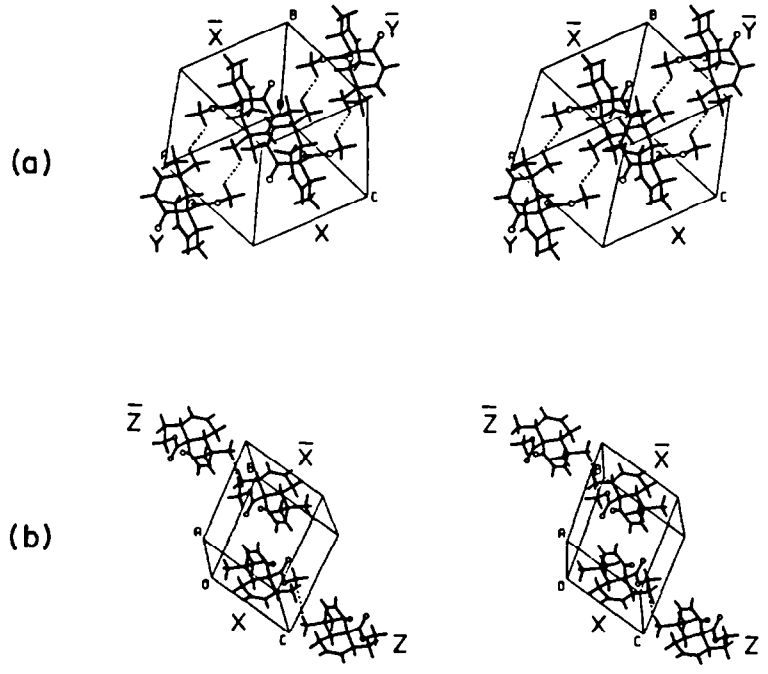

Figure 8. Packing diagrams of compound 2. The potentially reactive molecules are X and $\bar{X}$.
(a) Relevant lattice environment for the "center-to-center" mechanism. The dotted lines represent the intermolecular steric compression preventing X and $\bar{X}$ from approaching each other along the double bond center-to-center vector. Translation of X along a generates Y.
(b) Relevant lattice environment for the "twist" mechanism. The dotted lines represent the intermolecular steric compression preventing X and $\bar{X}$ from approaching each other by the twist mechanism. Translation of X along c generates Z.

head-to-tail fashion and are parallel, above one another, and only slightly offset along the double bond axis (0.52Å); the center-to-center distance is 3.79Å. Nevertheless, photolysis of single crystals of 2 for up to 40 hours at -16° to -18°C (to prevent melting) with a Liconix Helium-Cadmium 325nm CW laser showed less than 1% reaction by capillary gas chromatography. This lack of reactivity is not an intrinsic property of enone 2, as irradiation in solution at the same wavelength leads to essentially quantitative yields of the cage compound (10) resulting from intramolecular [2+2] cycloaddition (Figure 9).

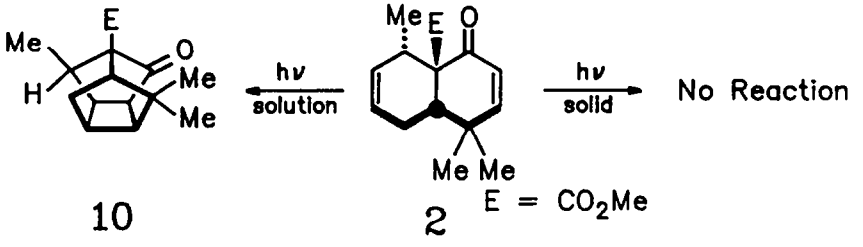

Figure 9. Anomalous solid state photoreactivity of compound 2.

Computer simulation of the solid state [2+2] photocycloaddition was carried out assuming two types of mechanism, center-to-center dimerization (I) and twist dimerization (II); in both cases the lattice environment was kept fixed while only the coordinates of the potentially reactive molecules X and $\bar{X}$ (Figure 8) were changed during the hypothetical dimerization. At each state of dimerization the new H...H contacts were determined using the previously mentioned INDIS3 computer program. It was found that along the reaction coordinate, whether following mechanism type (I) or (II), there are short intermolecular H...H contacts developed, arising from a methyl group on a stationary molecule impeding a methyl group on the reacting molecule. Eight methyl groups are involved in the steric compression along mechanism (I) [Figure 8(a)], four methyl groups are involved in type (II) [Figure 8(b)]. The interacting methyl groups on both the reacting molecule X and the stationary molecule Y were rotated in both directions by 30° and the new intermolecular H...H contacts were determined. As in the case of enones 1a-1h, the overall conclusions are not altered when rotation of the interacting methyl groups is taken into account.

(I) "Center-to-Center" Photodimerization Mechanism

Two reaction pathways were considered; (Ia) Molecules X and $\bar{X}$ move toward each other in 0.24Å increments along the double bond center-to-center vector (dual motion mechanism) and (Ib) molecule $\bar{X}$ remains fixed while molecule X moves toward it in 0.48Å increments (single motion mechanism). By virtue of the symmetry of the system, all four H...H contacts are identical, and the contacts developed by moving X toward $\bar{X}$ are the same as those developed by moving $\bar{X}$ toward X.

The results are shown graphically in Figure 10. This is a plot of the total steric compression energy (MMP2) versus double bond center-to-center distance for both the dual motion and single motion dimerization pathways. In both cases, the steric compression accompanying dimerization is of sufficient magnitude to account reasonably for the lack of dimerization. For example, at a center-to-center distance of 2.35Å, the shortest H...H contact is 1.9Å and the total MMP2 repulsion energy of four such contacts is 13.2 Kcal/mole.

This corresponds to a pre-dimerization geometry in which 2p-2p orbital overlap is small [based on Roberts' calculations of the overlap integral S_{ij} versus distance for 2p-σ and 2p-π bonding[33]]. Using these data, we estimate that at a center-to-center separation of 2.35Å (offset 0.33Å), the p-orbital overlap between molecules X and $\bar{X}$ is less than 20% of maximum. Further movement towards each other becomes prohibitively expensive owing to the fact that the H...H repulsion energy rises very steeply below 1.9Å (Figure 5).

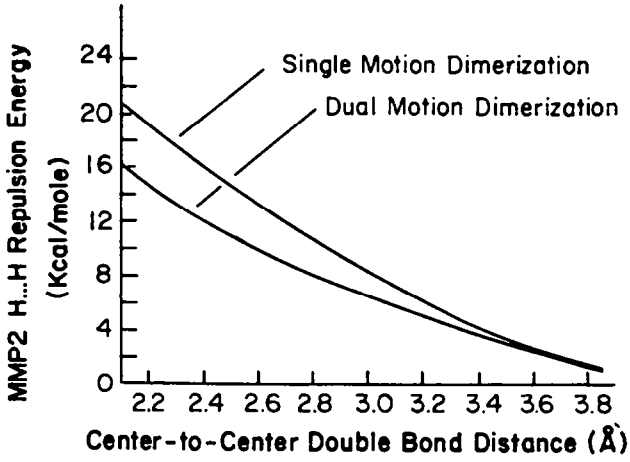

Figure 10. Total repulsion energy vs. distance in attempted dimerization.

The computer simulation of the "center-to-center" photodimerization mechanism shows that the steric hindrance between the interacting methyl groups reaches a maximum when the two double bonds are 2.1Å apart. At a center-to-center distance above 2.1Å, the dual motion photodimerization is less sterically hindered than the single motion pathway. Figure 11 is an idealized drawing of the packing arangement for compound 2 showing the methyl-methyl interactions relevant for the "center-to-center" mechanism. Simply put, the sum of four interactions developed in moving both reactants toward each other by a distance d is less than the sum of the two much more severe interactions which result when one of the reactants is moved toward the other by a distance 2d.

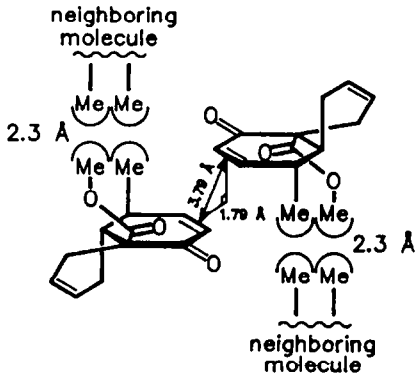

Figure 11. Steric compression inhibition of solid state photodimerization along the "center-to-center" mechanism.

(II) "Twist" Photodimerization Mechanism

Two such mechanisms were considered: (IIa) Molecules X and $\bar{X}$ are each rotated around the intramolecular C1...C4 vector in 5° intervals (dual "twist" mechanism), and (IIb) molecule $\bar{X}$ remains fixed while molecule X is rotated around its C1...C4 vector in 5° intervals (single "twist" mechanism). By virtue of the symmetry of the system, the two H...H contacts are identical, and the contacts developed by twisting X are the same as those developed by twisting $\bar{X}$.

The idealized drawing of the packing arrangement for compound 2 relevant for the "twist" mechanism is shown in Figure 12. At a 20° counterclockwise twist, the center-to-center distance decreases from 3.79Å to 3.16Å, and the 2.3Å H...H intermolecular contacts are decreased to 1.64 and 1.72Å (the total 6-12 repulsion energy is 52.8 Kcal/mole); at the same time the offset between the 2p orbitals increases from 1.79Å to 2.65Å, a less favored geometry for dimerization. A single motion "twist" mechanism in which $\bar{X}$ is fixed while only molecule X is rotated around its C1...C4 vector is even worse (with respect to the possibility of dimerization), since the 2p orbitals will no longer be parallel to each other. As before, the overall conclusions are not altered when rotations of the interacting methyl groups are taken into account.

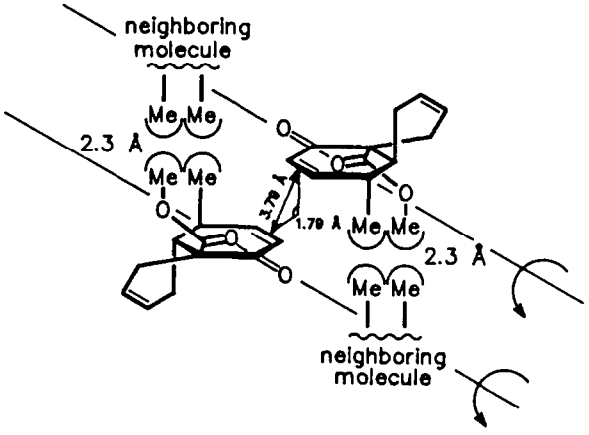

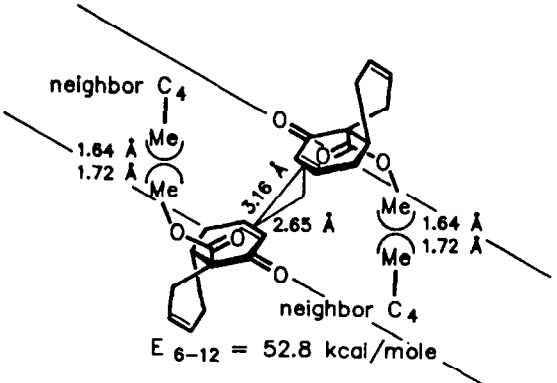

Figure 12. Possible "twist" photodimerization mechanism.
Top: Idealized drawing of the packing arrangement of compound 2 showing the Me...Me interactions.
Bottom: Idealized drawing of the cycloaddition geometry after 20° counterclockwise twist of both molecules X and $\bar{X}$.

(C) INTRAMOLECULAR STERIC COMPRESSION: REGIOSELECTIVITY

Based on our experience with ene-dione 11[34-35] (Figure 13) it seemed likely that ene-dione 3 would exist in solution as a nearly 1:1 mixture of conformers A and B (Figure 14). A solid state magic angle spinning C-13 NMR spectrum[36] and a single crystal X-ray diffraction study[37] show that ene-dione 3 exists in a single conformation A in the solid state.

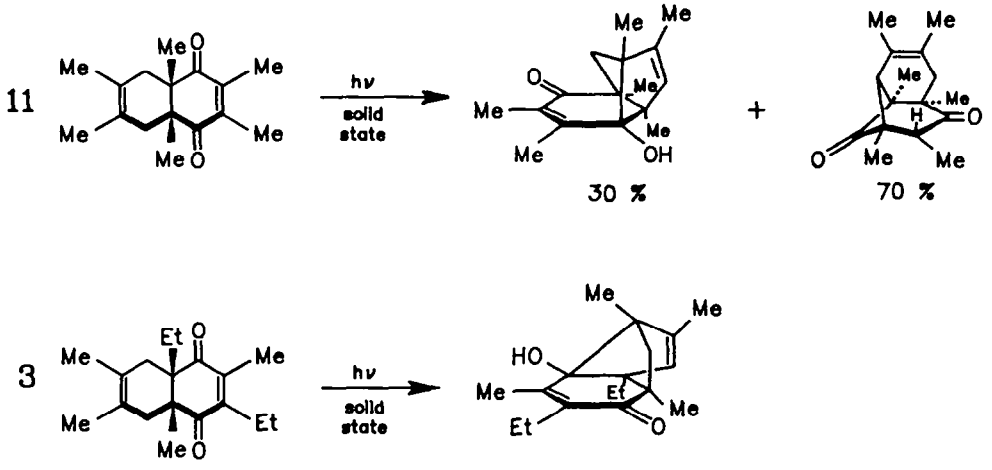

Figure 13. Solid state photochemistry of ene-diones.

Irradiation of ene-dione 11, both in solution and in the solid state, gives enone alcohol (30%) and cyclobutanone (70%), both processes being topochemically allowed[38]. Since for 11 $R_1=R_2=CH_3$, whether the starting conformation is A or B does not change the product, as A'=B', and A"=B". In the case of ene-dione 3, however, $R_1=CH_3$, $R_2=C_2H_5$, thus A' and B' are not identical nor are A" and B". Thus in the solid state, photolysis of 3 should give only A' and/or A" because only conformer A is present; irradiation in solution would be expected to provide a mixture of all four isomers.

This is what is found experimentally. Irradiation of ene-dione 3 with the output from a Molectron UV 22 nitrogen laser (337 nm) gives only enone alcohol A', whereas laser photolysis of benzene or acetonitrile solutions of the same material affords mixtures of products: A', B', A" and B", the composition depending on the length of irradiation[39].

The observation of a single photoproduct, enone alcohol A', in the solid state irradiation of ene-dione 3, is very interesting. This was unexpected because in our previous work on the solid state photochemistry of ene-dione 11, enone alcohol A' was found to be the minor product, with cyclobutanone A" predominating. We attribute these results to an unfavorable solid state steric effect accompanying attempted cyclobutanone formation in the

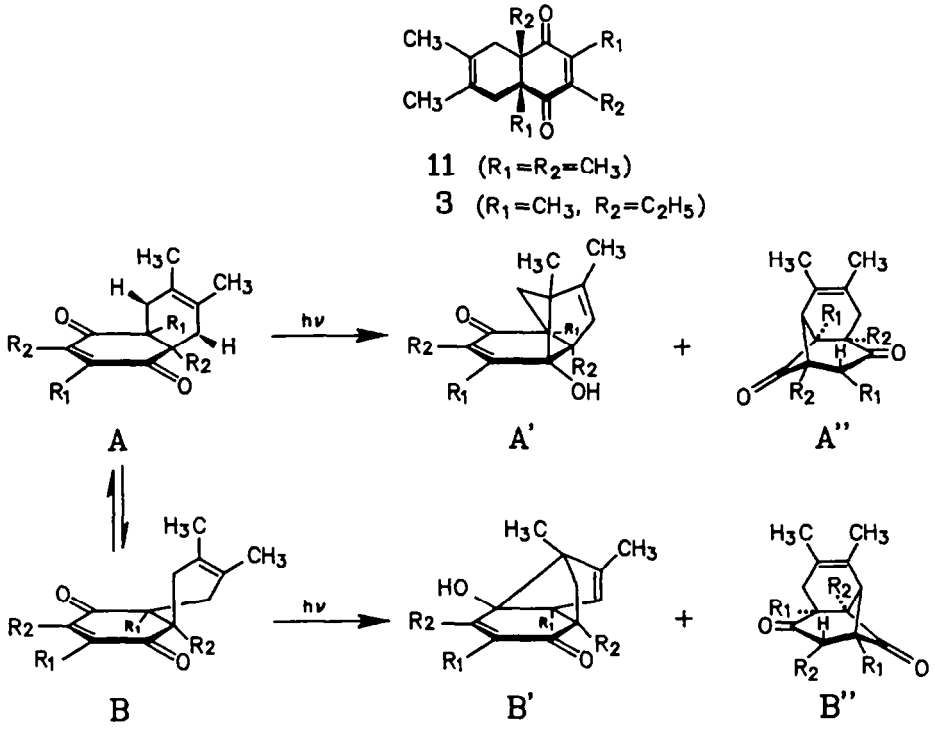

Figure 14. Ene-dione conformations A and B, and the possible products upon photolysis.

case of compound 3, but not for compound 11. Specifically, we suggest that steric compression retards the rate of the first step of cyclobutanone formation, transfer of hydrogen to the enone carbon, in the case of compound 3, but not 11 (Figure 15, top). Hydrogen transfer to the enone carbon requires a change of the hybridization of the carbon from sp^2 to sp^3, and the steric compression developed, shown by dotted lines in Figure 15, involves two unfavorable intramolecular methyl...methyl interactions between the downward-moving methyl group and its intramolecular neighboring ethyl groups. When the neighboring groups are methyl (i.e. ene-dione 11), no such interactions exist.

Computer simulation of the pyramidalization of the above carbon was performed (Figure 15, bottom) in a way similar to that already described for compound 1. The shortest intramolecular H...H contacts, 1.58 and 1.75Å, were calculated for the geomtery of full pyramidalization. The corresponding total non-bonded repulsion energy, using the Lennard-Jones 6-12 potential[16], is 35 Kcal/mole.

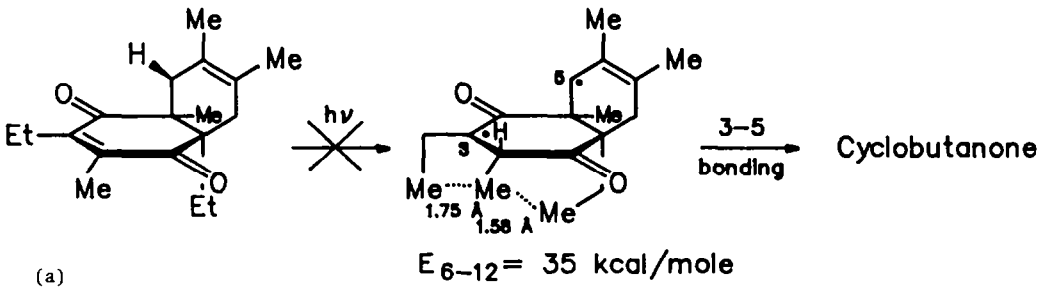

(a)

E_{6-12} = 35 kcal/mole

(b)

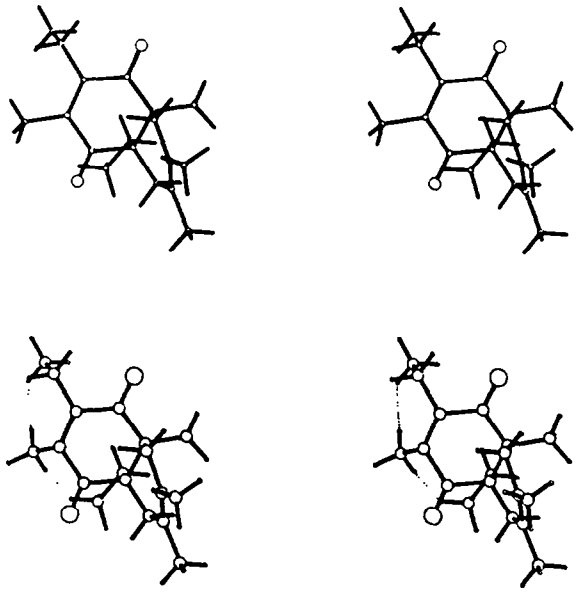

Figure 15. Hydrogen abstraction by carbon in compound 3 involving intramolecular steric compression.
(a) Idealized drawing of the steric compression arising from the hydrogen transfer. Steric compression is absent when all six substituents are methyl.
(b) Computer simulation of the change of hybridization of the enone carbon. Upper: before pyramidalization. Lower: after pyramidalization.

Methyl group rotation was checked for the three methyl groups involved, the non-stationary methyl group and the two stationary methyl groups. Rotation of the stationary methyl groups does not change the conclusions of the above steric compression. However, rotation of the non-stationary methyl group at its fully pyramidalized position, plotted in Figure 16, is very interesting. This plot shows that although the intramolecular steric compression is indeed released upon rotation of the non-stationary methyl group, new intermolecular steric compression is introduced into the lattice system from two short intermolecular H...H contacts.

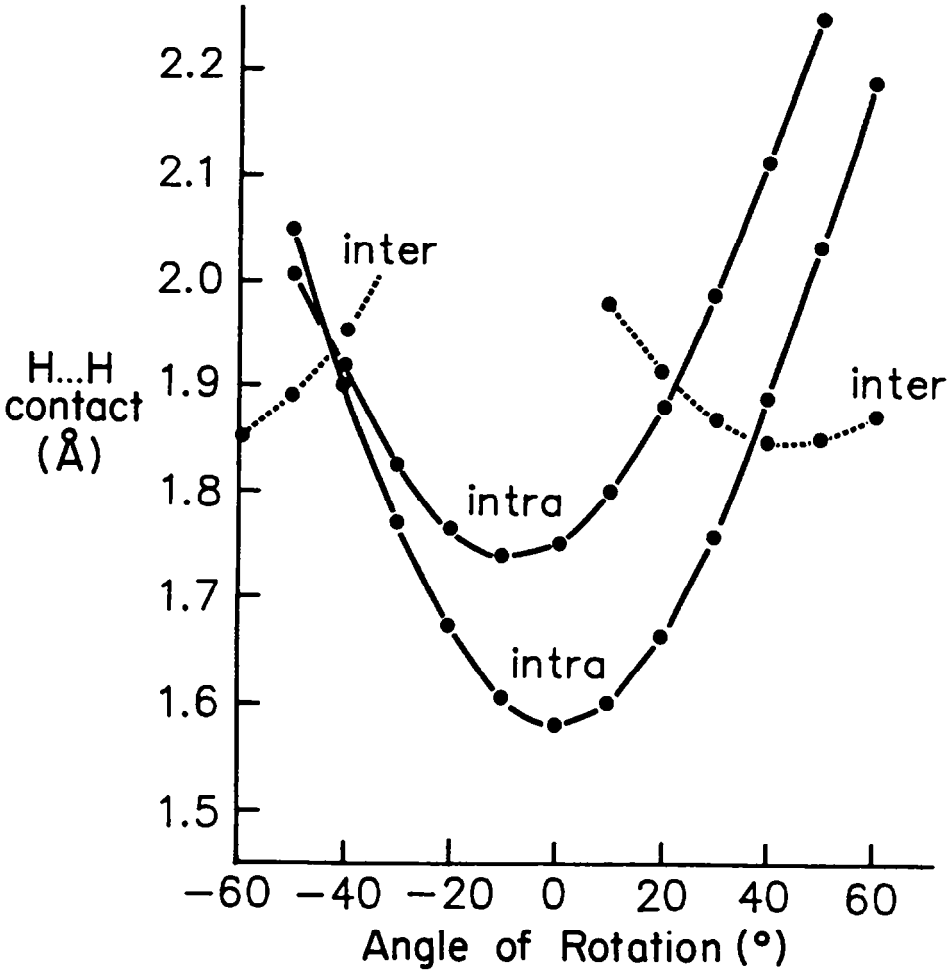

Figure 16. Non-bonded H...H contacts versus angle of rotation of the non-stationary methyl group at its fully pyramidalized position.

If we assume that the solution conformation of compound 3 is similar to its solid state conformation, Figure 16 explains the solution photoproducts beautifully: the new intermolecular H...H contacts arising from rotating the non-stationary methyl group do not exist in solution, thus the steric compression is relieved and hydrogen abstraction by the enone carbon can take place. Furthermore, ethyl group rotation is less restricted in solution than in the solid state, and the intramolecular steric compression can be avoided to permit cyclobutanone formation in solution (as observed).

EXPERIMENTAL

General

IR spectra were recorded on Perkin-Elmer 137, 457 or 710 B spectrometers. The spectra of liquids were recorded neat or as 10% solutions in chloroform; solids were determined using KBr pellets containing 1 mg of sample in 200 mg of KBr. Proton NMR spectra were recorded on Varian EM-360L, HA-100 and XL-100 spectrometers, or on Brüker WH-400 or WP-80 instruments; tetramethylsilane was used as internal standard. Mass spectra were obtained either on an Atlas CH-4B spectrometer (low resolution) or on a Kratos MS-50 instrument (high and low resolution). Both instruments were operated at an ionizing potential of 70 eV. UV spectra were recorded on a Carey 15 spectrophotometer. Elemental analyses were performed by the departmental microanalyst, Mr. P. Borda. Melting points were determined on a Fischer-Johns hot-stage apparatus, or for solids which sublimed, on a Gallenkamp instrument in sealed capillary tubes; all melting points are uncorrected. Thin layer chromatography was carried out using silica gel 60F-254 on pre-coated aluminum sheets from E. Merck. Vapor phase chromatography was conducted on a Hewlett-Packard model 5830-A packed column instrument with nitrogen as the carrier gas.

The details of the preparation and photochemistry of hydroxy-enones 1a-1f have been reported previously[6]. Included in the present paper for the first time are the experimental details for acetoxy-enones 1g and 1h.

Preparation of 2,3,4aβ,6,7,8aβ-Hexamethyl-4a,5,8,8a-tetrahydronaphthoquin-1-on-4α-acetate(1g)

A solution of 0.90g (3.0 mmoles) of hydroxy-enone 1a[6] in 6 mℓ of anhydrous pyridine and 3 mℓ of freshly distilled acetic anhydride was stirred at room temperature under nitrogen for 8 hours. The reaction mixture was diluted with water and extracted twice with chloroform. The organic extracts were washed with 1M HCℓ, saturated sodium bicarbonate solution, and water. After drying, the solvent was removed in vacuo to give a light yellow liquid. Column chromatography (silica gel, 20% ethyl acetate-petroleum ether) afforded acetoxy-enone 1g (0.98g, 96%) as a colorless oil, which formed large, clear crystals when dissolved in a small volume of hexane and set aside at -10°C for 24 hours. Mp 67.5-68.5°C; IR (KBr) 1736, 1675 (C=O) cm^{-1}; NMR ($CDCℓ_3$) δ 0.95(s, 3H, CH_3), 1.07 (s, 3H, CH_3), 1.28-2.88 (m, 4H), 1.55 (br s, 3H, C(6) or C(7) CH_3), 1.60 (br s, 3H, C(6) or C(7) CH_3), 1.80 (s, 6H, C(2) and C(3) CH_3's), 2.20 (s, 3H, acetate CH_3), 5.85 (br s, 1H, -CHOAc); mass spectrum m/e 290(M^+); UV max ($CHCℓ_3$) sh 330 nm (ε 64).

Anal. Calcd. for $C_{18}H_{26}O_3$: C, 74.45; H, 9.02
Found: C, 74.47; H, 9.05

Photolysis of Acetoxy-Enone 1g in Benzene

A degassed solution of 122 mg (0.42 mmoles) of acetoxy-enone 1g in 180 mℓ of purified benzene was photolyzed through a uranium glass filter sleeve (λ>340nm) using a 450 W Hanovia medium pressure mercury lamp. After 4.5 hours tℓc indicated complete reaction and formation of a single photoproduct. Removal of benzene in vacuo gave a yellow solid which was dissolved in petroleum ether-ethanol, filtered to remove insoluble material, and cooled to -10°C, whereupon needles of the intramolecular [2+2] cage compound 5-exo-acetoxy-1,3,4,6,8,9-hexamethyltetracyclo [4.4.0.0.^{3,9}0^{4,8}]decan-2-one were deposited (106mg, 87%). Mp 148.5-150° (sealed tube); IR (KBr) 1733 (C=O) cm^{-1}; NMR ($CDCℓ_3$) δ 0.76 (d, 1H, J=12 Hz), 0.85 (s, 3H, CH_3), 0.91 (s, 3H, CH_3), 0.93 (s, 3H, CH_3), 0.96 (s, 3H, CH_3), 1.04 (s, 6H, CH_3's), 1.40 (d, 1H, J=12 Hz), 1.98 (d, 1H, J=12 Hz), 2.04 (s, 3H, acetate CH_3), 2.13 (d, 1H, J=12 Hz), 4.61 (s, 1H, -CH OAC); mass spectrum m/e 290 (M^+); UV max ($CHCℓ_3$) 298 nm (ε 36).

Anal. Calcd. for $C_{18}H_{26}O_3$: C, 74.45; H, 9.02
Found: C, 74.47; H, 9.10

This material (20mg, 0.07 mmoles) was hydrolyzed in 2 mℓ of methanol containing 10 mg of anhydrous potassium carbonate (room temperature, 10 hours). The solution was diluted with water, extracted with chloroform, and the chloroform solution dried over magnesium sulfate. Removal of solvent in vacuo yielded a white solid which was a single product by gℓc and showed an IR spectrum and mp identical to that for the cage keto-alcohol formed by solution photolysis of hydroxy-enone 1a[6].

Photolysis of Acetoxy-Enone 1g in the Solid State

Crystals of acetoxy-enone 1g (118 mg) were deposited on the reaction surface of a specially constructed solid state photolysis apparatus[38] and irradiated at -39°C for 5 hours with light of wavelength >340 nm. Extensive column chromatography of the reaction mixture (silica gel, 20% ethyl acetate-petroleum ether) afforded 16 mg of a new photoproduct (subsequently identified as 9g) plus 98 mg of recovered 1g. Compound 9g was further purified by short path, Kugelrohr distillation at 0.1 Torr and 90°C. IR (liquid film) 1742, 1715 (C=O) cm^{-1}; NMR ($CDCℓ_3$) δ 0.90 (s, 3H, CH_3), 1.01 (s, 3H, CH_3), 1.05 (s, 3H, CH_3), 1.08 (d, 3H, J=7 Hz), $CHCH_3$), 1.55 (s, 6H, vinyl CH_3's), 1.85 (d, 1H, J=16 Hz), 2.07-2.21 (m, 2H), 2.16 (s, 3H, acetate CH_3), 2.41 (br s, 1H), 4.59 (s, 1H, -CH OAc); mass spectrum m/e 290 (M^+);

UV max ($CHCl_3$) sh 300 nm (ε 63).

Anal. Calcd. for $C_{18}H_{26}O_3$: C, 74.45; H, 9.02
Found: C, 74.24; H, 8.95

Compound 9g (7 mg) was converted to the corresponding keto-alcohol using potassium carbonate in methanol as previously described. Without purification, the resulting oil was dissolved in 3 mℓ of methylene chloride and treated with 14 mg of pyridinium chlorochromate. After stirring at room temperature for 3 hours, work up, column chromatography (20% ethyl acetate-petroleum ether) and short path distillation yielded 92% of an oil whose IR and NMR spectra were identical to the known[40] diketone 9g (R_3 and R_4 = 0).

Preparation of 2,3,4aβ,6,7,8aβ-Hexamethyl-4a,5,8,8a-tetrahydronaphthoquin-1-on-4β-acetate (1h)

A solution of 0.84 g (2.9 mmoles) of hydroxy-enone 1b[6] in 6 mℓ of dry pyridine and 3 mℓ of freshly distilled acetic anahydride was stirred at room temperature under nitrogen for 12 hours. Workup as for compound 1g afforded 0.93g (95%) of colorless oil which solidified. Recrystallization form a minimum amount of hexane at -10°C gave large, clear prisms. Mp 77-77.5°C; IR (KBr) 1739, 1667 (C=O) cm^{-1}; NMR ($CDCl_3$) δ 0.90 (s, 3H, CH_3), 1.10 (s, 3H, CH_3), 1.37-2.70 (m, 4H), 1.50 (br s, 3H, C(6) or C(7) CH_3), 1.57 (br s, 3H, C(6) or C(7) CH_3) 1.80 (s, 6H, C(2) and C(3) CH_3), 2.15 (s, 3H, acetate CH_3), 5.73 (br s, 1H, -CHOAc); mass spectrum m/e 290 (M^+); UV max ($CHCl_3$) 237 nm (ε 11,500), sh 325 nm (ε 62).

Anal. Calcd. for $C_{18}H_{26}O_3$: C, 74.45; H, 9.02
Found: C, 74.30; H, 9.00

Photolysis of Acetoxy-Enone 1h in Benzene

A solution of 214 mg (0.74 mmoles) of acetoxy-enone 1h in 250 mℓ of benzene was photolyzed as in the case of 1g for 6 hours. After removal of solvent in vacuo and crystallization from hexane, long, colorless needles (76 mg, 36%) of intramolecular [2+2] cage photoproduct 5-endo-acetoxy-1,3,4,6,8,9-hexamethyltetracyclo-[4.4.0.0.^{3,9} $0^{4,8}$]decan-2-one were deposited. Mp 137.5-138°C (sealed tube); IR (KBr) 1733 (C=O) cm^{-1}; NMR ($CDCl_3$) δ 0.62 (d, 1H, J=13 Hz), 0.91 (s, 3H, CH_3), 0.93 (s, 3H, CH_3), 0.96 (s, 3H, CH_3), 1.01 (m, 1H), 1.03 (s, 3H, CH_3), 1.04 (s, 3H, CH_3), 1.07 (s, 3H, CH_3), 2.00 (d, 1H, J=13 Hz), 2.01 (s, 3H, acetate CH_3), 2.07 (d, 1H, J=13 Hz), 4.50 (s, 1H, -CHOAc); mass spectrum m/e 290 (M^+); UV max ($CHCl_3$) 290 nm (ε 42).

Anal. Calcd. for $C_{18}H_{26}O_3$: C, 74.45; H, 9.02
Found: C, 74.30; H, 9.02

Hydrolysis of the cage photoproduct as described previously afforded material which was identical in every respect with the photoproduct formed from phtolysis of hydroxy-enone 1b in benzene[6].

The photolysis mixture mother liquor was concentrated and subjected to preparative glc (5' x 1/4" column, 8% OV-17 on 80/100 Chromosorb W, 200°C, 120 mℓ/min). This afforded a further 54 mg (25%) of cage photoproduct plus 21 mg (10%) of a second photoproduct tentatively identified as 2,3,4aβ,6β,7,8aβ-hexamethyl-4a,5,6,8a-tetrahydronaphthoquin-1-on-4β-acetate, a double bond isomer of 1h.

Photolysis of Acetoxy-Enone 1h in the Solid State

Crystals of acetoxy-enone 1h (110 mg, 0.38 mmoles) were irradiated for 2.3 hours at -14°C in the apparatus described previously[38]. Silica gel column chromatography (20% ethyl acetate-petroleum ether) afforded 75 mg of residual starting material and 31 mg of a new photoproduct identified as 8h. This material was purified by Kugelrohr distillation (85°C, 0.1 Torr) and crystallized from a very small volume of hexane at -10°C. Mp 124.5-125.5°C; IR (KBr) 1761, 1736 (C=O) cm^{-1}; NMR ($CDCl_3$) δ 0.83 (d, 3H, J=7 Hz, $-CHCH_3$), 0.87 (s, 3H, CH_3), 1.04 (s, 3H, CH_3) 1.12 (s, 3H, CH_3), 1.61 (br s, 3H, vinyl CH_3), 1.64 (s, 1H), 1.73 (br s, 3H, vinyl CH_3), 1.79 (d, 1H, J=18 Hz), 2.0 (s, 3H, acetate CH_3) 2.21 (d, 1H, J=18 Hz), 2.43 (m, 1H), 4.76 (d, 1H, J=5 Hz, -CHOAc); mass spectrum m/e 290 (M^+); UV max ($CHCl_3$) 287 nm (ε 64).

Anal. Calcd. for $C_{18}H_{26}O_3$: C, 74.45; H, 9.02
Found: C, 74.60; H, 9.18

Photolysis of Enone 2

A solution of 10 mg (0.04 mmoles) of enone 2 in 10 mℓ of benzene was photolyzed for 40 minutes using a 450 W Hanovia medium pressure mercury lamp fitted with a Pyrex filter sleeve. Solvent was removed in vacuo and the remaining oil crystallized from low boiling petroleum ether to afford colorless crystals of intramolecular [2+2] cage compound 10 (8 mg, 80%). Mp 52-53°C; IR ($CHCl_3$) 1745, 1720 (C=O) cm^{-1}; NMR ($CDCl_3$) δ 0.87 (m, 6H, CH_3 and $CHCH_3$); 1.30 (s, 3H, CH_3), 1.58-3.25 (m, 8H), 3.80 (s, 3H, $-OCH_3$); high resolution mass spectrum calculated for $C_{15}H_{20}O_3$: 248.1412; found 248.1411.

Acknowledgement

We thank the Natural Sciences and Engineering Research Council of Canada for financial support. We are grateful to Professor H-J. Liu of the University of Alberta for a generous sample of enone 2.

References

1. Cohen, M.D.; Schmidt, G.M.J. J. Chem. Soc. 1964, 1996-2000.

2. Cohen, M.D. Angew. Chem., Int. Ed. Engl. 1975, 14, 386-93.

3. McBride, J.M. Acc. Chem. Res. 1983, 16, 304-12.

4. Gavezzotti, A. J. Am. Chem. Soc. 1983, 105, 5220-5.

5. Ariel, S.; Askari, S.; Scheffer, J.R.; Trotter, J.; Walsh, L. J. Am. Chem. Soc. 1984, 106 5726-8.

6. Appel, W.K.; Jiang, Z.Q.; Scheffer, J.R.; Walsh, L. J. Am. Chem. Soc. 1983, 105, 5354-63.

7. Compounds 1a and 1b: Greenhough T.J.; Trotter, J. Acta Cryst. 1980, B36, 1831-5.

8. Compound 1c: Secco, A.S.; Trotter, J. Acta Cryst. 1982, B38, 2190-6.

9. Compound 1d: Greenhough, T.J.; Trotter, J. Acta Cryst. 1980, B36, 2843-6.

10. Compound 1e: Greenhough, T.J.; Trotter, J. Acta Cryst. 1980, B36, 1835-9.

11. Compound 1f: Secco, A.S.; Trotter, J. Acta Cryst. 1982, B38, 1233-7.

12. Compounds 1g and 1h: Ariel, S.; Trotter, J. Acta Cryst. 1985, C41, 295-8.

13. Pienta, N.J. J. Am. Chem. Soc. 1984, 106, 2704-5.

14. Schuster, D.I.; Bonneau, R.; Dunn, D.A.; Rao, J.M.; Joussot-Dubien, J. J. Am. Chem. Soc. 1984, 106, 2706-7.

15. Local program at the Dept. of Structural Chemistry, the Weizmann Institute of Science, Rehovot, Isreal.

16. Hagler, A.T.; Sharon, R. CMIN2 program. 1973. Dept. of Chem. Phys. The Weizmann Institute of Science, Rehovot, Isreal.

17. Allinger, N.L.; Spraque, J.T. J. Am. Chem. Soc. 1973, 95, 3893-907.

18. Wagner, P.J. Top. Curr. Chem. 1976, 66, 1-52.

19. Wagner, P.J. In "Rearragements in Ground and Excited States"; de Mayo, P., Ed.; Academic: New York, 1980; Vol. 3, pp 381-444.

20. Scaiano, J.C.; Lissi, E.A.; Encina, M.V. Rev. Chem. Intermed. 1978, 2, 139-96.

21. Scaiano, J.C.; Acc. Chem. Res. 1982, 15, 252-8.

22. Wagner, P.J. Acc. Chem. Res. 1971, 4, 168-77.

23. Schmidt, G.M.J. Pure Appl. Chem. 1971, 27, 647-78.

24. Schmidt, G.M.J. "Solid State Photochemistry"; Ginsburg, D., Ed.; Verlag Chemie, New York, 1976.

25. Thomas, J.M.; Morsi, S.E.; Desvergne, J.P. In "Advances in Physical Organic Chemistry"; Academic: New York, 1977; Vol. 15.

26. Thomas, J.M. Pure Appl. Chem. 1979, 51, 1065-82.

27. Lahav, M.; Green, B.S.; Rabinovich, D. Acc. Chem. Res. 1979, 12, 191-7.

28. Scheffer, J.R. Acc. Chem. Res. 1980, 13, 283-90.

29. Addadi, L.; Ariel, S.; Lahav, M.; Leiserowitz, L.; Popovitz-Biro, R.; Tang, C.P. In "Chemical Physics of Solids and Their Surfaces"; Roberts, M.W.; Thomas, J.M., Eds.; The Royal Society of Chemistry: London, 1980; Specialist Periodical Reports, Vol. 8; Ch. 7.

30. Byrn, S.R. "The Solid State Chemistry of Drugs"; Academic, New York, 1982.

31. Hasegawa, M. Chem. Rev. 1983, 83, 507-18.

32. Synthesis: Brown, E.N.C. Ph.D. thesis, University of Alberta, Canada, 1980. Crystal Structure: Ariel, S.; Trotter, J. Acta Cryst. 1984, C40, 2084-6.

33. Roberts, J.D. "Molecular Orbital Calculations"; Benjamin, New York, 1961; p. 30.

34. X-ray crystal structure: Phillips, S.E.V.; Trotter, J. Acta Cryst. 1976, B32, 3088-91.

35. CPMAS C-13 solid state NMR: McDowell, C.A.; Naito, A.; Scheffer, J.R.; Wong, Y-F. Tett. Lett. 1981, 22, 4779-82.

36. Ariel, S.; Scheffer, J.R.; Trotter, J.; Wong, Y-F. Tett. Lett. 1983, 24, 4555-8.

37. Evans, S.V.; Hwang, C.; Trotter, J. 1985, unpublished results.

38. Scheffer, J.R.; Dzakpasu, A.A. J. Am. Chem. Soc. 1978, 100, 2163-73.

39. Ariel, S.; Evans, S.V.; Hwang, C.; Jay, J.; Scheffer, J.R.; Trotter, J.; Wong, Y-F. Tett. Lett. 1985, 26, 965-8.

40. Scheffer, J.R.; Bhandari, K.S.; Gayler, R.E.; Wostradowski, R.A. J. Am. Chem. Soc. 1975, 97, 2178.